

Supplementary Information

Chemically monodispersed tin nanoparticles on monolithic 3D nanoporous copper for lithium ion battery anodes with ultralong cycle life and stable lithium storage

Wenbo Liu,^{a,*} Xue Chen,^a Peng Xiang,^a Shichao Zhang,^b Jiazen Yan,^a Ning Li,^a
Sanqiang Shi^c

^a School of Manufacturing Science and Engineering, Sichuan University, Chengdu
610065, China

^b School of Materials Science and Engineering, Beihang University, Beijing 100191,
China

^c Department of Mechanical Engineering, The Hong Kong Polytechnic University,
Hung Hom, Kowloon, Hong Kong

Tel: +86-028-85405320; Fax: +86-028-85403408; E-mail: liwenbo_8338@163.com.

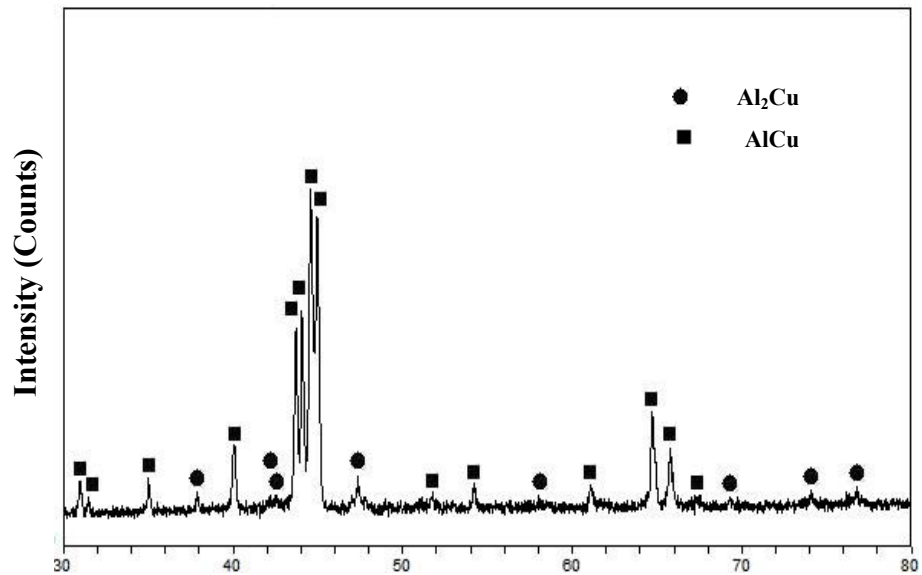


Figure S1. The XRD pattern of the initial Al 45 at.% Cu alloy sheets.

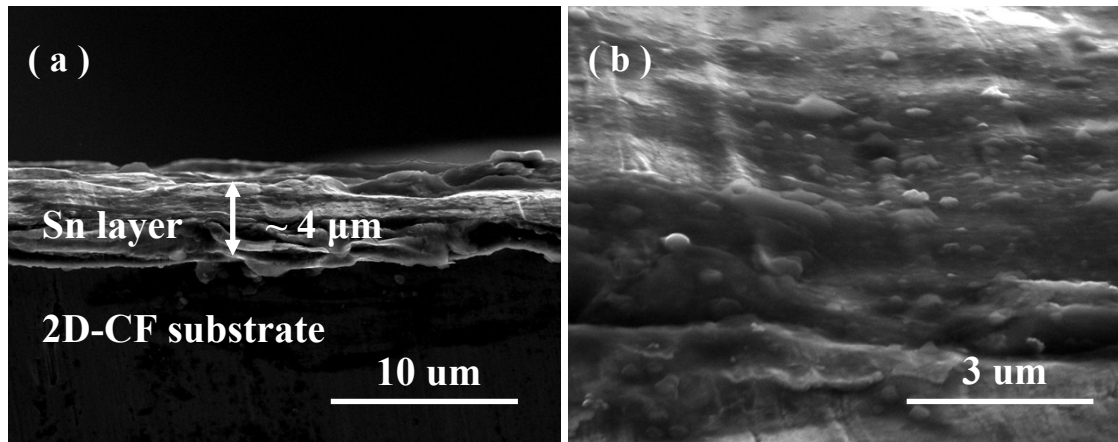


Figure S2. SEM images showing the cross-section microstructures of 2D-CF@TTFs composite after electroless plating tin at the low temperature, in which parts b is the high-magnification image.

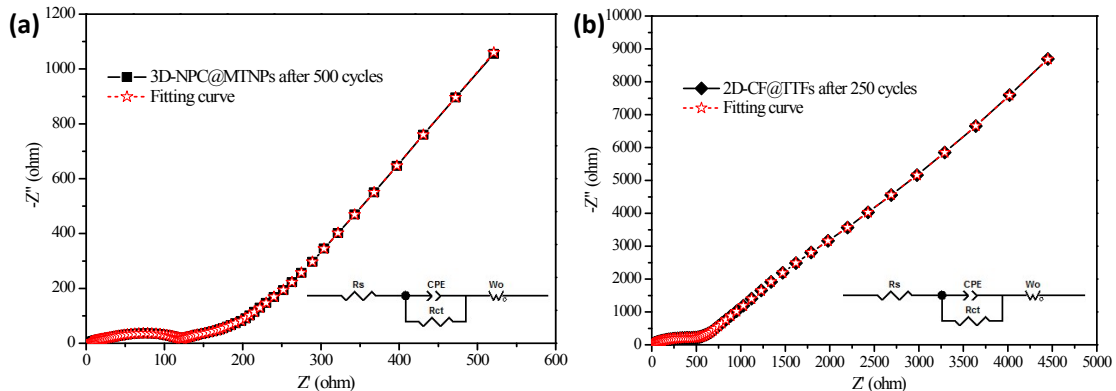


Figure S3. Nyquist plots of (a) 3D-NPC@MTNPs electrode after 500 charge-discharge cycles and (b) 2D-CF@TTFs electrode after 250 charge-discharge cycles. The insets in parts a and b are their relevant fitting circuits.

As indicated clearly in Figure S3, the fitting curves of the 3D-NPC@MTNPs and 2D-CF@TTFs electrodes after cyclings are in good agreement with their EIS results. Meanwhile, the equivalent circuits for fitting are displayed in the insets of Figure S3, comprising the typical circuit models including the electrolyte resistance R_s , charge transfer resistance R_{ct} , Warburg impedance of Li^+ diffusion in electrode W_o , and space charge capacitance at electrode/electrolyte interface CPE. The present experimental results reveal the 3D-NPC@MTNPs electrode have significantly lower R_s ($3.1\ \Omega$) and R_{ct} ($106\ \Omega$) after 500 long-cycles than those of 2D-CF@TTFs electrode just after 250 cycles ($R_s=5.1\ \Omega$, $R_{ct}=821\ \Omega$), indicating that the unique 3D-NPC@MTNPs composite as anode for LIBs possesses much better Li^+ and electron transport abilities.

Table S1. Chemical composition of the initial Al-Cu alloy sheets by EDX analysis.

Specimens	Elements (at.%)
-----------	-----------------

	Al	Cu
Initial Al-Cu alloy sheets	54.68	45.32

Table S2. A detailed comparison of lithium storage property of various Sn and Sn-based composites with different structure designs.

Materials	Structure	Capacity	Cycles	Capacity retention	Ref.
Sn	nanoparticle	1.29 mAh cm ⁻²	100	35.4 %	1
SnO ₂ /Cu ₁₀ Sn ₃ /Cu	powder	0.25 mAh cm ⁻²	50	45.5 %	2
Sn	nanoparticle	0.93 mAh cm ⁻²	100	64.1 %	3
SnS ₂ /CN	naoflower	0.42 mAh cm ⁻²	200	60.5 %	4
Sn/SnO ₂	nanoparticle	1.09 mAh cm ⁻²	100	60.2 %	5
Sn-Ni	nanoparticle	0.25 mAh cm ⁻²	200	51 %	6
SnSb/N-C	nanosheet	0.32 mAh cm ⁻²	100	70.6 %	7
C@Sn@C	nanofiber	0.14 mAh cm ⁻²	100	62.2 %	8
CF/Sn SnO ₂ @C	submicron particle	1.84 mAh cm ⁻²	50	76.5 %	9
Sn-Cu	nanotube	465 mAh g ⁻¹	100	50.5 %	10
Cu ₆ Sn ₅ /Cu	nanoporous	326 mAh g ⁻¹	50	41.5 %	11
Sn/C	nanoparticle	284.6 mAh g ⁻¹	250	31.1 %	12
Sn	nanoparticle	0.485 mAh cm ⁻²	500	52.4 %	Our work

References

- 1 Luo et al. *Mater. Lett.*, 2018, **213**, 189-192.
- 2 Park et al. *Appl. Surf. Sci.*, 2017, **399**, 132-138.
- 3 Luo et al. *ACS Appl. Mater. Inter.*, 2018, **10**, 22050-22058.
- 4 Yin et al. *Electrochim. Acta*, 2019, **293**, 408-418.
- 5 Wang et al. *Electrochim. Acta*, 2018, **292**, 72-80.
- 6 Dong et al. *Chem. Eng. J.*, 2018, **350**, 791-798.
- 7 Pan et al. *Chem. Eng. J.*, 2018, **348**, 653 – 660.
- 8 Huang et al. *Chem. Eng. J.*, 2018, **344**, 625 – 632.
- 9 Yang et al. *J. Alloy Compd.*, 2018, **750**, 220-227.
- 10 Xu et al. *Appl. Surf. Sci.*, 2017, **423**, 245-254.
- 11 Xing et al. *Micropor. Mesopor. Mat.*, 2018, **261**, 237-243.
- 12 Guler et al. *Appl. Surf. Sci.*, 2018, **446**, 122-130.